ACS OMEGA
http://pubs.acs.org/journal/acsodf Article

Defect Engineering of Hafnia-Based Ferroelectric Materials for High-Endurance Memory Applications

Min-Kyu Kim,[†] Ik-Jyae Kim,[†] and Jang-Sik Lee*

Cite This: *ACS Omega* 2023, 8, 18180−18185

Read Online

ACCESS | Metrics & More | Article Recommendations | Supporting Information

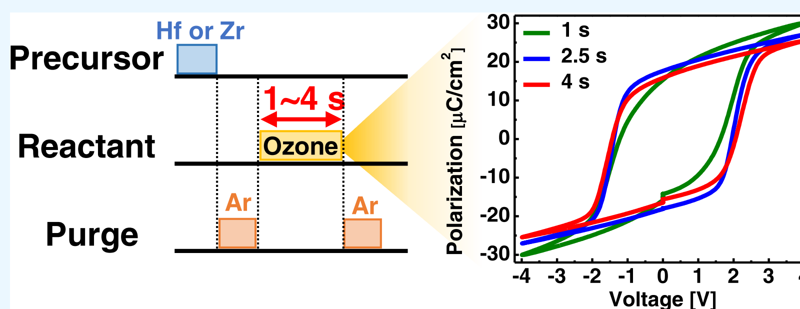

ABSTRACT: Zirconium-doped hafnium oxide ($HfZrO_x$) is one of the promising ferroelectric materials for next-generation memory applications. To realize high-performance $HfZrO_x$ for next-generation memory applications, the formation of defects in $HfZrO_x$, including oxygen vacancies and interstitials, needs to be optimized, as it can affect the polarization and endurance characteristics of $HfZrO_x$. In this study, we investigated the effects of ozone exposure time during the atomic layer deposition (ALD) process on the polarization and endurance characteristics of 16-nm-thick $HfZrO_x$. $HfZrO_x$ films showed different polarization and endurance characteristics depending on the ozone exposure time. $HfZrO_x$ deposited using the ozone exposure time of 1 s showed small polarization and large defect concentration. The increase of the ozone exposure time to 2.5 s could reduce the defect concentration and improve the polarization characteristics of $HfZrO_x$. When the ozone exposure time further increased to 4 s, a reduction of polarization was observed in $HfZrO_x$ due to the formation of oxygen interstitials and non-ferroelectric monoclinic phases. $HfZrO_x$, with an ozone exposure time of 2.5 s, exhibited the most stable endurance characteristics because of the low initial defect concentration in $HfZrO_x$, which was confirmed by the leakage current analysis. This study shows that the ozone exposure time of ALD needs to be controlled to optimize the formation of defects in $HfZrO_x$ films for the improvement of polarization and endurance characteristics.

■ INTRODUCTION

Ferroelectric materials based on hafnium oxide have the potential to overcome the limitations of perovskite-based ferroelectric materials because of their several advantages, including a low process temperature, high scalability, and complementary metal-oxide-semiconductor compatibility.[1−4] Due to these advantages, zirconium-doped hafnium oxide ($HfZrO_x$) has been used as a ferroelectric material for negative capacitance transistors, next-generation memory devices, and neuromorphic devices.[5−10] However, $HfZrO_x$ has shown a limitation in endurance characteristics compared with perovskite-based ferroelectric materials.[11−14] The degradation of $HfZrO_x$ under repeated electrical stress is due to the generation and accumulation of defects.[14,15] Therefore, to improve the endurance characteristics, optimization of the defects in $HfZrO_x$ is required.[16,17]

The formation of defects in $HfZrO_x$ can be affected by the types of electrodes, annealing temperature, and ozone exposure time of the atomic layer deposition (ALD) process.[14,18,19] In particular, the ozone exposure time may be a critical parameter to the formation of oxygen defects in $HfZrO_x$, such as oxygen vacancy and interstitial defects because ozone reacts with the Hf and Zr precursors to form the $HfZrO_x$ layer during the ALD process.[19] These defects can affect the leakage current and breakdown of $HfZrO_x$ during operation. Previously, it was shown that the formation of the non-ferroelectric monoclinic phase could be suppressed and the growth of the ferroelectric orthorhombic phase could be promoted by optimizing the ozone exposure time.[19−22] Also, due to different phase compositions, the ferroelectric characteristics such as remnant polarization and coercive electric field could be affected by the ozone exposure time.[21,22] However, most of the previous

Received: March 8, 2023
Accepted: April 24, 2023
Published: May 8, 2023

© 2023 The Authors. Published by American Chemical Society

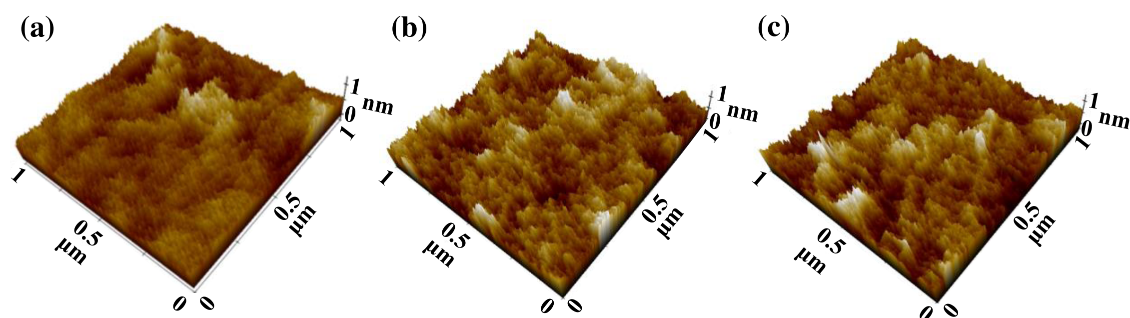

Figure 1. Topography images measured by atomic force microscope of $HfZrO_x$ films with the different ozone exposure times of (a) 1 s, (b) 2.5 s, and (c) 4 s.

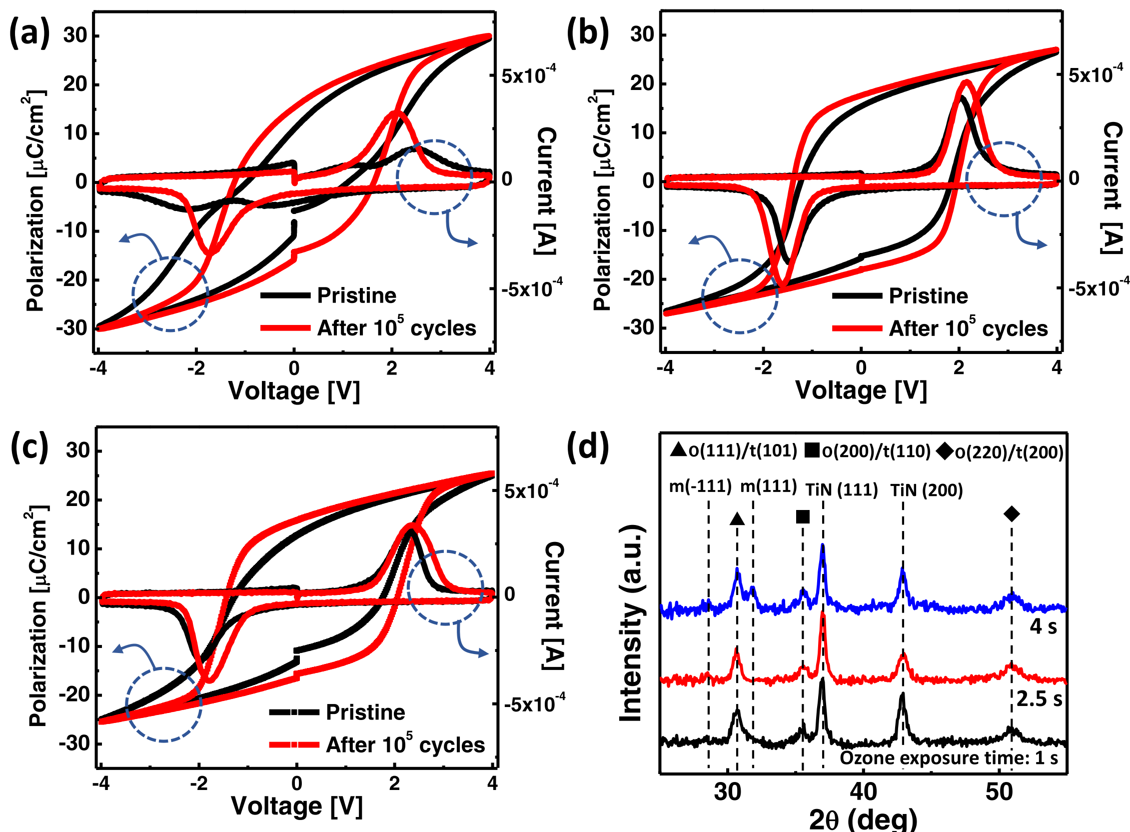

Figure 2. Polarization−voltage (left *y*-axis) and current−voltage curves (right *y*-axis) of $HfZrO_x$ deposited using ozone exposure times of (a) 1 s, (b) 2.5 s, and (c) 4 s at the pristine state and after 10^5 bipolar pulse cycles. (d) GIXRD patterns with a 2θ range of 25−55° of $HfZrO_x$ films deposited using the ozone exposure times of 1, 2.5, and 4 s.

studies analyzed the effect of ozone exposure time on the defect and electrical properties of thin $HfZrO_x$ films with a thickness of <10 nm.[19−22] The impact of the ozone exposure time may be different in thicker $HfZrO_x$ films due to different in-plane stress induced in the films.[23] Also, as thicker $HfZrO_x$ films are beneficial for memory applications due to their large memory window, the effect of ozone exposure on the defect and electrical properties of $HfZrO_x$ should be further analyzed.

In this study, we investigate the polarization and endurance characteristics of a 16-nm-thick $HfZrO_x$ according to the ozone exposure time. When the ozone exposure time increases from 1 to 2.5 s, a wake-up effect is reduced and the polarization characteristics of $HfZrO_x$ are improved. A longer ozone exposure time of 4 s induces the reduction of polarization in $HfZrO_x$. The effect of the ozone exposure time on the endurance characteristics of $HfZrO_x$ is investigated. The optimized ozone exposure time (2.5 s) improves the endurance characteristics of $HfZrO_x$ by reducing the defects in $HfZrO_x$. These results show that optimization of the ozone exposure time is essential to improve the ferroelectric and endurance characteristics of $HfZrO_x$.

■ RESULTS AND DISCUSSION

In this study, a 16-nm-thick $HfZrO_x$ is used, which can provide a sufficient memory window for memory device applications. As the memory window of the ferroelectric transistor is directly related to the coercive field and thickness of the ferroelectric layer, a thicker HZO is used to achieve a larger memory window.[24,25] The morphology of $HfZrO_x$ films with different ozone exposure times was investigated (Figure 1). The root-mean-square (RMS) roughness of $HfZrO_x$ films with ozone exposure times of 1, 2.5, and 4 s were 0.297, 0.412, and 0.428

https://doi.org/10.1021/acsomega.3c01561
ACS Omega 2023, 8, 18180−18185

nm, respectively, which confirmed the uniform and conformal growth of $HfZrO_x$ films. The RMS roughness increased when the ozone exposure time increased, which could be originated from different phase compositions.[26,27]

The polarization−voltage and switching current−voltage curves of ferroelectric capacitors with the TiN/$HfZrO_x$/TiN structure based on different ozone exposure times were measured. When analyzing $HfZrO_x$ with the ozone exposure time of 1 s, antiferroelectric characteristics were observed at the pristine state.[28,29] The ferroelectric polarization curve was observed after 10^5 bipolar rectangular pulse cycles using a voltage pulse with an amplitude of ±4 V, width of 5 μs, and rise/fall time of 100 ns. In the polarization curve with a 4-V sweep, the positive- ($+P_r$) and negative-remnant polarization ($-P_r$) were 12.6 and −14.4 μC/cm^2, respectively (Figure 2a). With an ozone exposure time of 2.5 s, $HfZrO_x$ showed ferroelectric polarization characteristics at the pristine state. After 10^5 bipolar pulse cycles, $+P_r$ and $-P_r$ were 17.4 and −17.2 μC/cm^2, respectively, which are larger than those of $HfZrO_x$ with an ozone exposure time of 1 s (Figure 2b). When the ozone exposure time increased to 4 s, the ferroelectric polarization characteristics were still observed at the pristine states. However, $+P_r$ and $-P_r$ obtained after 10^5 bipolar pulse cycles decreased to 15.1 and −15.3 μC/cm^2, respectively (Figure 2c). These results indicated that the ozone exposure time could affect the phase composition of $HfZrO_x$.[19−22] To confirm the effects of ozone exposure time on the phases of $HfZrO_x$, we analyzed the grazing incidence X-ray diffraction (GIXRD) patterns of $HfZrO_x$ films with the ozone exposure times of 1, 2.5, and 4 s (Figure 2d). In GIXRD patterns of all $HfZrO_x$ films, the peaks from the (111), (200), and (220) planes of the orthorhombic phases were observed, which were the origin of the ferroelectricity of $HfZrO_x$. These peaks could be a mixture of the orthorhombic and tetragonal phases of (101), (110), and (200) planes.[30,31] For $HfZrO_x$ films with ozone exposure times of 1 and 2.5 s, the peak from the monoclinic phase was not observed. However, when the long ozone exposure time (4 s) was used, the peak from the (111) plane of the monoclinic phase was observed (Figure S1). When the oxygen source (i.e. ozone) is overexposed, the monoclinic phase can be induced in $HfZrO_x$ films.[20−22] The formation of the monoclinic phase can reduce the polarization of $HfZrO_x$ films. Therefore, the ozone exposure time needs to be optimized to stabilize the ferroelectric orthorhombic phase.

The endurance characteristics of $HfZrO_x$ with different ozone exposure times were investigated. The devices underwent bipolar rectangular pulse cycles with a width of 5 μs, rise/fall time of 100 ns, and amplitudes of ±3, ±4, and ±5 V (±1.875, ±2.5, and ±3.125 MV/cm). The properties of the devices were measured before and after applying the bipolar pulse cycles. The $HfZrO_x$ deposited using the ozone exposure time of 2.5 s exhibited the most stable endurance characteristics. With the ozone exposure time of 1 s, $HfZrO_x$ showed a large increment of polarization during the repeated switching operation, which was called as the wake-up effect (Figure 3a). With a higher voltage, polarization increased, but the endurance characteristics were degraded. When the ozone exposure time increased to 2.5 s, a large increment of polarization was not observed during cycles, and longer endurance cycles were observed (Figure 3b). When bipolar pulses with an amplitude of ±3 V were used, $HfZrO_x$ could achieve stable polarization characteristics for 10^9 cycles. The breakdown of the $HfZrO_x$ layer was observed after 5 × 10^9

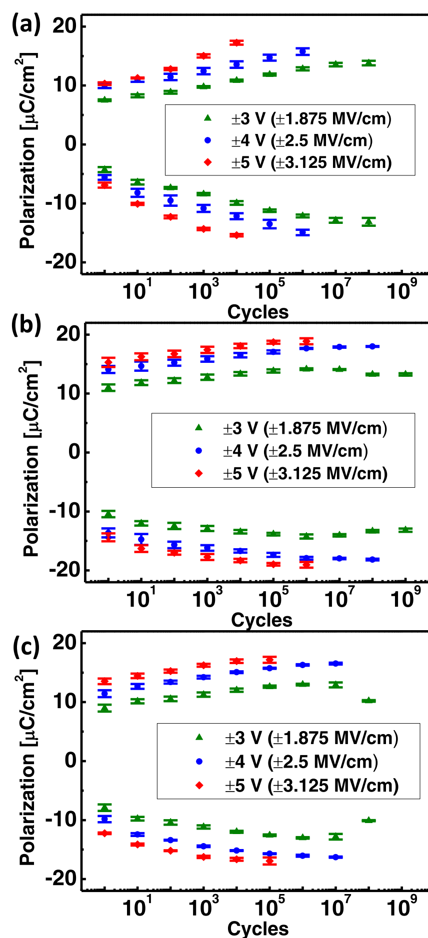

Figure 3. Endurance characteristics of $HfZrO_x$ deposited using ozone exposure times of (a) 1 s, (b) 2.5 s, and (c) 4 s (error bars: standard deviation from the measurement of five devices). Bipolar pulses with a width of 5 μs and amplitudes of 3, 4, and 5 V are used.

cycles. With the longer ozone exposure time of 4 s, a wake-up effect similar to $HfZrO_x$ with an ozone exposure time of 2.5 s was observed, which was smaller than $HfZrO_x$ with an ozone exposure time of 1 s. However, the endurance characteristics were degraded, and the breakdown of the $HfZrO_x$ layer was observed after 10^8 cycles (Figure 3c). These differences may originate from an increase in the defects, such as oxygen vacancies or interstitials in $HfZrO_x$.

To investigate the defect concentration and generation rate of $HfZrO_x$, leakage currents of $HfZrO_x$ films were analyzed depending on the voltage stress. After applying the voltage stress, leakage currents of $HfZrO_x$ films deposited using different ozone exposure times were measured (Figure 4a). The leakage current of $HfZrO_x$ films decreased with an increase in the voltage stress time. This behavior may originate from charge trapping by the newly generated oxygen defects.[32] The change of $I_{leakage}$ is defined as $\Delta I = I_{initial} - I$. Here, $I_{initial}$ and I are the leakage currents at the initial state and after applying the voltage stress pulse, respectively. To fit ΔI depending on the stress time, $\Delta I = \Delta I_0 t^{\gamma}$ was used.[32,33] Here, ΔI_0 is proportional to the initial defect concentration (i.e. defect concentration before the voltage stress) and γ represents the defect generation rate.[32−34] Ozone exposure time did not affect the defect generation rates of $HfZrO_x$. However, $HfZrO_x$ films showed different initial defect concentrations depending on the ozone exposure times (Figure 4b). $HfZrO_x$ with an

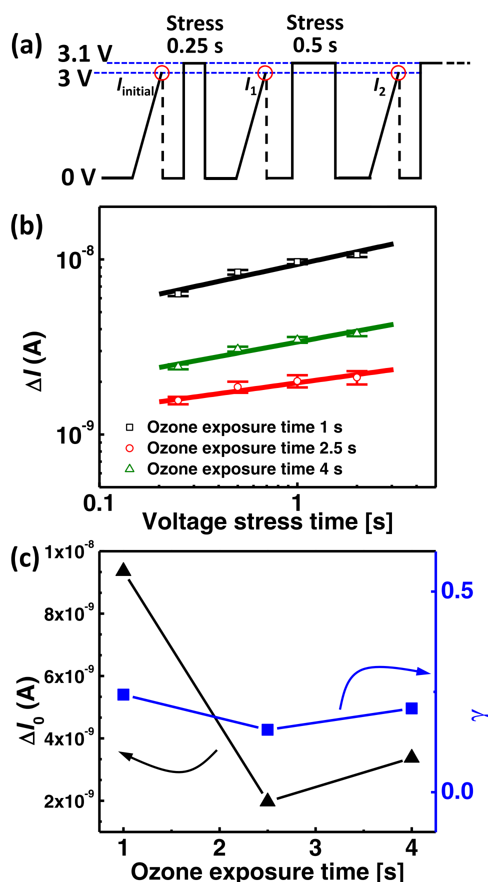

Figure 4. (a) Measurement sequence to evaluate the leakage current characteristics of $HfZrO_x$. (b) Change of leakage current (ΔI) according to the voltage stress time for $HfZrO_x$ deposited using different ozone exposure times (error bars: standard deviation from the measurement of 5 devices). (c) ΔI_0 and γ of $HfZrO_x$ according to the ozone exposure time.

ozone exposure time of 2.5 s showed a smaller initial defect concentration than $HfZrO_x$ with ozone exposure times of 1 and 4 s. $HfZrO_x$ films with short ozone exposure time (1 s) showed the largest initial defect concentration in analysis based on leakage current. When the ozone exposure time increased to 2.5 s, the initial defect concentration decreased, which may indicate a decrease in oxygen vacancy concentration. However, when the ozone exposure time was further increased to 4 s, the $HfZrO_x$ film showed a larger initial defect concentration than the $HfZrO_x$ film using the ozone exposure time of 2.5 s (Figure 4c). With overexposure to the oxygen source, defects, such as oxygen interstitials, can be seen in $HfZrO_x$ films.[35,36] Oxygen interstitials have been suggested as the origin of stabilizing the monoclinic phase in $HfZrO_x$ films.[37−39] $HfZrO_x$ film using the ozone exposure time of 4 s showed the peak of the monoclinic phase in GIXRD measurement and the increased initial defect concentration compared with $HfZrO_x$ film using the ozone exposure time of 2.5 s. The degraded endurance characteristics of $HfZrO_x$, with an increase in the ozone exposure time from 2.5 to 4 s, seem to be originated from the formation of oxygen interstitials. Therefore, the reason for the improved endurance characteristics of $HfZrO_x$, with an ozone exposure time of 2.5 s, seems to be the low initial defect concentration, including oxygen vacancies and interstitials. The low initial defect concentration can prevent the breakdown of the $HfZrO_x$ layer.[40] As the ALD is based on thermally activated chemical reactions, the defect concentration can also be affected by the deposition temperature, type of precursors, and reactants.[41−43] However, in this work, only the ozone exposure time during the deposition is changed, and all other parameters are fixed. Thus, the difference between HZO films is thought to be originated from the difference in the ozone exposure time, which can change the concentration of oxygen-related vacancies. In this work, we correlated the leakage current of the hafnia-based ferroelectric transistor with the defect inside the $HfZrO_x$ film. Although other sources, such as surface roughness, structural defect, and tunneling, could affect the leakage current, we excluded other sources due to the following reasons: First, if the surface roughness was the main contributor to the leakage current difference, the leakage current of the ferroelectric capacitor with a 4-s ozone exposure time should show the highest leakage current, but the ferroelectric capacitor with a 1-s ozone exposure time showed the highest leakage current. Also, structural defects, such as pin holes or pores, were excluded because the thin film was conformally deposited using ALD (Figure 1). Finally, as the thickness of the ferroelectric thin film used in this work was 16 nm, the direct tunneling through the ferroelectric thin film could be suppressed compared with ferroelectric films with a thinner thickness.[44] Thus, we believe that the main contributor to the leakage current is the oxygen-vacancy-related defects that originated from different ozone exposure times. These results indicate that the optimization of the ozone exposure time can reduce the initial defect concentration and lead to the improvement of endurance characteristics of $HfZrO_x$.

■ CONCLUSIONS

In summary, we investigated the effects of ozone exposure time in the ALD process on the ferroelectric and endurance characteristics of $HfZrO_x$. With the short ozone exposure time of 1 s, $HfZrO_x$ showed wake-up effects and large initial defect concentrations. When the ozone exposure time increased from 1 to 2.5 s, the wake-up effects and initial defect concentration of $HfZrO_x$ were reduced. The further increase of ozone exposure time could induce the formation of oxygen interstitials, which might cause the reduction of polarization. Among the ozone exposure condition (1−4 s), an ozone exposure time of 2.5 s showed the largest polarization and most stable endurance characteristics. These improved characteristics were achieved by the optimization of defects and phase composition in $HfZrO_x$ by controlling the ozone exposure time. This study provides a feasible strategy to improve the endurance and ferroelectric characteristics of $HfZrO_x$ by optimizing the ozone exposure time for promoting the application of $HfZrO_x$ to next-generation memory devices.

■ EXPERIMENTAL DETAILS

Materials. $Hf[N(C_2H_5)CH_3]_4$ [tetrakis(ethylmethylamido)hafnium (TEMAH)] and $Zr[N(C_2H_5)CH_3]_4$ [tetrakis(ethylmethylamido)zirconium (TEMAZ)] were purchased from UP Chemical, Korea. Si wafers with 100-nm-thick thermally grown SiO_2 were used as substrates.

Device Fabrication. Ferroelectric capacitors with a TiN/$HfZrO_x$/TiN structure were fabricated on the SiO_2/Si substrate. First, a 100-nm-thick TiN layer was deposited on the SiO_2/Si substrate using direct current sputtering. Then, the 16-nm-thick $HfZrO_x$ films were deposited via ALD using the HfO_2/ZrO_2 ALD cycle ratio of 1:1 at 280 °C. $Hf[N(C_2H_5)$-

$CH_3]_4$ (TEMAH), $Zr[N(C_2H_5)CH_3]_4$ (TEMAZ), and ozone with a concentration of 180 g/m^3 were used as Hf precursor, Zr precursor, and oxygen source, respectively.[5,10] The ozone was inserted into the chamber after Hf and Zr precursors were inserted. During the deposition of $HfZrO_x$, ozone exposure times of 1, 2.5, and 4 s were used. The 100-nm-thick TiN electrode formed on the $HfZrO_x$. Then, the ferroelectric characteristics of $HfZrO_x$ were induced by thermal annealing under an N_2 environment for 1 min at 500 °C. The area of the TiN top electrode was 50 μm × 50 μm.

Characterizations. All characteristics were measured at room temperature under ambient conditions. The polarization−voltage curves and endurance characteristics of $HfZrO_x$ with different ozone exposure times were measured using a pulse measurement unit (PMU) (4225-PMU, KEITHLEY Instruments). The leakage current characteristics of $HfZrO_x$ with different ozone exposure times were measured using a semiconductor parameter analyzer (4200A-SCS, KEITHLEY Instruments). The surface roughnesses of $HfZrO_x$ layers were measured by atomic force microscopy (Park Systems, NX10). The crystal structures of the $HfZrO_x$ films were analyzed using the grazing incidence X-ray diffraction (GIXRD) (D/MAX-2500, Rigaku).

ASSOCIATED CONTENT

Supporting Information

The Supporting Information is available free of charge at https://pubs.acs.org/doi/10.1021/acsomega.3c01561.

Additional data on GIXRD patterns for $HfZrO_x$ thin films (PDF)

AUTHOR INFORMATION

Corresponding Author

Jang-Sik Lee − *Department of Materials Science and Engineering, Pohang University of Science and Technology (POSTECH), Pohang 37673, Korea;* orcid.org/0000-0002-1096-1783; Email: jangsik@postech.ac.kr

Authors

Min-Kyu Kim − *Department of Materials Science and Engineering, Pohang University of Science and Technology (POSTECH), Pohang 37673, Korea*

Ik-Jyae Kim − *Department of Materials Science and Engineering, Pohang University of Science and Technology (POSTECH), Pohang 37673, Korea;* orcid.org/0000-0002-7560-6811

Complete contact information is available at: https://pubs.acs.org/10.1021/acsomega.3c01561

Author Contributions

[†]M.-K.K. and I.-J.K. contributed equally to this work. J.-S.L. conceived and directed the research. J.-S.L. and M.-K.K. designed and planned the experiment. M.-K.K. and I.-J.K. performed the experiment and acquired the data. M.-K.K., I.-J.K., and J.-S.L. wrote the manuscript.

Notes

The authors declare no competing financial interest.

ACKNOWLEDGMENTS

This work was supported by Samsung Research Funding & Incubation Center of Samsung Electronics under Project No. SRFC-TA1903-05. This work was also supported by the National Research Foundation of Korea (NRF-2019R1A2C2084114) and Samsung Electronics Company Ltd. (IO201215-08198-01).

REFERENCES

(1) Müller, J.; Böscke, T. S.; Schröder, U.; Mueller, S.; Bräuhaus, D.; Böttger, U.; Frey, L.; Mikolajick, T. Ferroelectricity in Simple Binary ZrO_2 and HfO_2. *Nano Lett.* **2012**, *12*, 4318−4323.

(2) Gong, N.; Ma, T. Why is FE−HfO_2 More Suitable than PZT or SBT for Scaled Nonvolatile 1-T Memory Cell? A Retention perspective. *IEEE Electron Device Lett.* **2016**, *37*, 1123−1126.

(3) Kim, S. J.; Mohan, J.; Summerfelt, S. R.; Kim, J. Ferroelectric $Hf_{0.5}Zr_{0.5}O_2$ Thin Films: A Review of Recent Advances. *JOM* **2019**, *71*, 246−255.

(4) Cheema, S. S.; Kwon, D.; Shanker, N.; dos Reis, R.; Hsu, S.-L.; Xiao, J.; Zhang, H.; Wagner, R.; Datar, A.; McCarter, M. R.; Serrao, C. R.; Yadav, A. K.; Karbasian, G.; Hsu, C.-H.; Tan, A. J.; Wang, L.-C.; Thakare, V.; Zhang, X.; Mehta, A.; Karapetrova, E.; Chopdekar, R. V.; Shafer, P.; Arenholz, E.; Hu, C.; Proksch, R.; Ramesh, R.; Ciston, J.; Salahuddin, S. Enhanced Ferroelectricity in Ultrathin Films Grown Directly on Silicon. *Nature* **2020**, *580*, 478−482.

(5) Kim, M.-K.; Lee, J.-S. Ferroelectric Analog Synaptic Transistors. *Nano Lett.* **2019**, *19*, 2044−2050.

(6) Khan, A. I.; Keshavarzi, A.; Datta, S. The Future of Ferroelectric Field-Effect Transistor Technology. *Nat. Electron.* **2020**, *3*, 588−597.

(7) Kim, M.-K.; Lee, J.-S. Synergistic Improvement of Long-Term Plasticity in Photonic Synapses Using Ferroelectric Polarization in Hafnia-Based Oxide-Semiconductor Transistors. *Adv. Mater.* **2020**, *32*, No. 1907826.

(8) Luo, Q.; Cheng, Y.; Yang, J.; Cao, R.; Ma, H.; Yang, Y.; Huang, R.; Wei, W.; Zheng, Y.; Gong, T.; Yu, J.; Xu, X.; Yuan, P.; Li, X.; Tai, L.; Yu, H.; Shang, D.; Liu, Q.; Yu, B.; Ren, Q.; Lv, H.; Liu, M. A Highly CMOS Compatible Hafnia-Based Ferroelectric Diode. *Nat. Commun.* **2020**, *11*, No. 1391.

(9) Kim, M.-K.; Kim, I.-J.; Lee, J.-S. Oxide Semiconductor-Based Ferroelectric Thin-Film Transistors for Advanced Neuromorphic Computing. *Appl. Phys. Lett.* **2021**, *118*, No. 032902.

(10) Kim, M.-K.; Kim, I.-J.; Lee, J.-S. CMOS-Compatible Ferroelectric NAND Flash Memory for High-Density, Low-Power, and High-Speed Three-Dimensional Memory. *Sci. Adv.* **2021**, *7*, No. eabe1341.

(11) Pešić, M.; Fengler, F. P. G.; Larcher, L.; Padovani, A.; Schenk, T.; Grimley, E. D.; Sang, X.; LeBeau, J. M.; Slesazeck, S.; Schroeder, U.; Mikolajick, T. Physical Mechanisms Behind the Field-Cycling Behavior of HfO_2-Based Ferroelectric Capacitors. *Adv. Funct. Mater.* **2016**, *26*, 4601−4612.

(12) Huang, F.; Chen, X.; Liang, X.; Qin, J.; Zhang, Y.; Huang, T.; Wang, Z.; Peng, B.; Zhou, P.; Lu, H.; Zhang, L.; Deng, L.; Liu, M.; Liu, Q.; Tian, H.; Bi, L. Fatigue Mechanism of Yttrium-Doped Hafnium Oxide Ferroelectric Thin Films Fabricated by Pulsed Laser Deposition. *Phys. Chem. Chem. Phys.* **2017**, *19*, 3486−3497.

(13) Chernikova, A. G.; Kozodaev, M. G.; Negrov, D. V.; Korostylev, E. V.; Park, M. H.; Schroeder, U.; Hwang, C. S.; Markeev, A. M. Improved Ferroelectric Switching Endurance of La-Doped $Hf_{0.5}Zr_{0.5}O_2$ Thin Films. *ACS Appl. Mater. Interfaces* **2018**, *10*, 2701−2708.

(14) Cao, R.; Song, B.; Shang, D.; Yang, Y.; Luo, Q.; Wu, S.; Li, Y.; Wang, Y.; Lv, H.; Liu, Q.; Liu, M. Improvement of Endurance in HZO-Based Ferroelectric Capacitor Using Ru Electrode. *IEEE Electron Device Lett.* **2019**, *40*, 1744−1747.

(15) Starschich, S.; Menzel, S.; Böttger, U. Pulse Wake-Up and Breakdown Investigation of Ferroelectric Yttrium Doped HfO_2. *J. Appl. Phys.* **2017**, *121*, No. 154102.

(16) Celano, U.; Chen, Y. H.; Minj, A.; Banerjee, K.; Ronchi, N.; McMitchell, S.; Marcke, P. V.; Favia, P.; Wu, T. L.; Kaczer, B.; Bosch, G. V.; Houdt, J. V.; Heide, P. *Probing the Evolution of Electrically Active Defects in Doped Ferroelectric HfO_2 During Wake-Up and Fatigue*, IEEE Symposium on VLSI Technology, June 6−19, 2020; pp 1−2.

https://doi.org/10.1021/acsomega.3c01561
ACS Omega 2023, 8, 18180−18185

(17) Islamov, D. R.; Zalyalov, T. M.; Orlov, O. M.; Gritsenko, V. A.; Krasnikov, G. Y. Impact of Oxygen Vacancy on the Ferroelectric Properties of Lanthanum-Doped Hafnium Oxide. *Appl. Phys. Lett.* **2020**, *117*, No. 162901.

(18) Yoon, S.-J.; Na, S.-Y.; Moon, S.-E.; Yoon, S.-M. Polarization Switching Kinetics of the Ferroelectric Al-Doped HfO_2 Thin Films Prepared by Atomic Layer Deposition with Different Ozone Doses. *J. Vac. Sci. Technol. B* **2019**, *37*, No. 050601.

(19) Kashir, A.; Oh, S.; Hwang, H. Defect Engineering to Achieve Wake-Up Free HfO_2-Based Ferroelectrics. *Adv. Eng. Mater.* **2021**, *23*, No. 2000791.

(20) Hoffmann, M.; Schroeder, U.; Schenk, T.; Shimizu, T.; Funakubo, H.; Sakata, O.; Pohl, D.; Drescher, M.; Adelmann, C.; Materlik, R.; Kersch, A.; Mikolajick, T. Stabilizing the Ferroelectric Phase in Doped Hafnium Oxide. *J. Appl. Phys.* **2015**, *118*, No. 072006.

(21) Pal, A.; Narasimhan, V. K.; Weeks, S.; Littau, K.; Pramanik, D.; Chiang, T. Enhancing Ferroelectricity in Dopant-Free Hafnium Oxide. *Appl. Phys. Lett.* **2017**, *110*, No. 022903.

(22) Mittmann, T.; Materano, M.; Chang, S. C.; Karpov, I.; Mikolajick, T.; Schroeder, U. *Impact of Oxygen Vacancy Content in Ferroelectric HZO Films on the Device Performance*, IEEE International Electron Devices Meeting (IEDM), December 12−18, 2020; pp 18.4.1−18.4.4.

(23) Xu, B.; Collins, L.; Holsgrove, K. M.; Mikolajick, T.; Schroeder, U.; Lomenzo, P. D. Influence of the Ozone Dose Time during Atomic Layer Deposition on the Ferroelectric and Pyroelectric Properties of 45 nm-Thick ZrO_2 Films. *ACS Appl. Electron. Mater.* **2023**, *5*, 2288−2295.

(24) Lue, H.-T.; Chien-Jang, W.; Tseung-Yuen, T. Device modeling of ferroelectric memory field-effect transistor (FeMFET). *IEEE Trans. Electron Devices* **2002**, *49*, 1790−1798.

(25) Mulaosmanovic, H.; Breyer, E. T.; Mikolajick, T.; Slesazeck, S. Ferroelectric FETs With 20-nm-Thick HfO_2 Layer for Large Memory Window and High Performance. *IEEE Trans. Electron Devices* **2019**, *66*, 3828−3833.

(26) Fields, S. S.; Cai, T.; Jaszewski, S. T.; Salanova, A.; Mimura, T.; Heinrich, H. H.; Henry, M. D.; Kelley, K. P.; Sheldon, B. W.; Ihlefeld, J. F. Origin of Ferroelectric Phase Stabilization via the Clamping Effect in Ferroelectric Hafnium Zirconium Oxide Thin Films. *Adv. Electron. Mater.* **2022**, *8*, No. 2200601.

(27) Lederer, M.; Kämpfe, T.; Olivo, R.; Lehninger, D.; Mart, C.; Kirbach, S.; Ali, T.; Polakowski, P.; Roy, L.; Seidel, K. Local Crystallographic Phase Detection and Texture Mapping in Ferroelectric Zr Doped HfO_2 Films by Transmission-EBSD. *Appl. Phys. Lett.* **2019**, *115*, No. 222902.

(28) Park, M. H.; Kim, H. J.; Kim, Y. J.; Lee, Y. H.; Moon, T.; Kim, K. D.; Hyun, S. D.; Hwang, C. S. Study on the Size Effect in $Hf_{0.5}Zr_{0.5}O_2$ Films Thinner than 8 nm Before and After Wake-Up Field Cycling. *Appl. Phys. Lett.* **2015**, *107*, No. 192907.

(29) Park, M. H.; Kim, H. J.; Lee, Y. H.; Kim, Y. J.; Moon, T.; Kim, K. D.; Hyun, S. D.; Hwang, C. S. Two-Step Polarization Switching Mediated by a Nonpolar Intermediate Phase in $Hf_{0.4}Zr_{0.6}O_2$ Thin Films. *Nanoscale* **2016**, *8*, 13898−13907.

(30) Wang, J.; Wang, D.; Li, Q.; Zhang, A.; Gao, D.; Guo, M.; Feng, J.; Fan, Z.; Chen, D.; Qin, M.; Zeng, M.; Gao, X.; Zhou, G.; Lu, X.; Liu, J. Excellent Ferroelectric Properties of $Hf_{0.5}Zr_{0.5}O_2$ Thin Films Induced by Al_2O_3 Dielectric Layer. *IEEE Electron Device Lett.* **2019**, *40*, 1937−1940.

(31) Park, M. H.; Kim, H. J.; Kim, Y. J.; Lee, W.; Moon, T.; Hwang, C. S. Evolution of Phases and Ferroelectric Properties of Thin $Hf_{0.5}Zr_{0.5}O_2$ Films According to the Thickness and Annealing Temperature. *Appl. Phys. Lett.* **2013**, *102*, No. 242905.

(32) Wei, W.; Zhang, W.; Wang, F.; Ma, X.; Wang, Q.; Sang, P.; Zhan, X.; Li, Y.; Tai, L.; Luo, Q.; Lv, H.; Chen, J. *Deep Insights Into the Failure Mechanisms in Field-Cycled Ferroelectric $Hf_{0.5}Zr_{0.5}O_2$ Thin Film: TDDB Characterizations and First-Principles Calculations*, IEEE International Electron Devices Meeting (IEDM), December 12−18, 2020; pp 39.6.1−39.6.4.

(33) Ichihara, R.; Fujii, S.; Yamaguchi, M.; Yoshimura, Y.; Mitani, Y.; Saitoh, M. Investigation of Switching-Induced Local Defects in Oxide-Based CBRAM Using Expanded Analytical Model of TDDB. *IEEE Trans. Electron Devices* **2019**, *66*, 2165−2171.

(34) Hirano, I.; Nakasaki, Y.; Fukatsu, S.; Masada, A.; Mitani, Y.; Goto, M.; Nagatomo, K.; Inumiya, S.; Sekine, K. *Impact of Metal Gate Electrode on Weibull Distribution of TDDB in HfSiON Gate Dielectrics*, IEEE International Reliability Physics Symposium, April 26−30, 2009; pp 355−361.

(35) Januar, M.; Prakoso, S. P.; Lan, S.-Y.; Mahanty, R. K.; Kuo, S.-Y.; Liu, K.-C. The Role of Oxygen Plasma in the Formation of Oxygen Defects in HfO_x Films Deposited at Room Temperature. *J. Mater. Chem. C* **2015**, *3*, 4104−4114.

(36) Bhuyian, M. N.; Sengupta, R.; Vurikiti, P.; Misra, D. Oxygen Vacancy Defect Engineering Using Atomic Layer Deposited $HfAlO_x$ in Multi-Layered Gate Stack. *Appl. Phys. Lett.* **2016**, *108*, No. 183501.

(37) Materano, M.; Mittmann, T.; Lomenzo, P. D.; Zhou, C.; Jones, J. L.; Falkowski, M.; Kersch, A.; Mikolajick, T.; Schroeder, U. Influence of Oxygen Content on the Structure and Reliability of Ferroelectric $Hf_xZr_{1-x}O_2$ Layers. *ACS Appl. Electron. Mater.* **2020**, *2*, 3618−3626.

(38) Materano, M.; Lomenzo, P. D.; Kersch, A.; Park, M. H.; Mikolajick, T.; Schroeder, U. Interplay between Oxygen Defects and Dopants: Effect on Structure and Performance of HfO_2-Based Ferroelectrics. *Inorg. Chem. Front.* **2021**, *8*, 2650−2672.

(39) Mittmann, T.; Michailow, M.; Lomenzo, P. D.; Gärtner, J.; Falkowski, M.; Kersch, A.; Mikolajick, T.; Schroeder, U. Stabilizing the Ferroelectric Phase in HfO_2-Based Films Sputtered from Ceramic Targets Under Ambient Oxygen. *Nanoscale* **2021**, *13*, 912−921.

(40) Florent, K.; Subirats, A.; Lavizzari, S.; Degraeve, R.; Celano, U.; Kaczer, B.; Piazza, L. D.; Popovici, M.; Groeseneken, G.; Houdt, J. V.*Investigation of the Endurance of FE-HfO_2 Devices by Means of TDDB Studies*, IEEE International Reliability Physics Symposium (IRPS), March 11−15, 2018; pp 6D.3-1−6D.3-7.

(41) Kim, K. D.; Park, M. H.; Kim, H. J.; Kim, Y. J.; Moon, T.; Lee, Y. H.; Hyun, S. D.; Gwon, T.; Hwang, C. S. Ferroelectricity in Undoped-HfO_2 Thin Films Induced by Deposition Temperature Control During Atomic Layer Deposition. *J. Mater. Chem. C* **2016**, *4*, 6864−6872.

(42) Kim, B. S.; Hyun, S. D.; Moon, T.; Do Kim, K.; Lee, Y. H.; Park, H. W.; Lee, Y. B.; Roh, J.; Kim, B. Y.; Kim, H. H.; Park, M. H.; Hwang, C. S. A Comparative Study on the Ferroelectric Performances in Atomic Layer Deposited $Hf_{0.5}Zr_{0.5}O_2$ Thin Films Using Tetrakis-(ethylmethylamino) and Tetrakis(dimethylamino) Precursors. *Nanoscale Res. Lett.* **2020**, *15*, 72.

(43) Kim, S. J.; Mohan, J.; Kim, H. S.; Lee, J.; Hwang, S. M.; Narayan, D.; Lee, J.-G.; Young, C. D.; Colombo, L.; Goodman, G.; Wan, A. S.; Cha, P.-R.; Summerfelt, S. R.; San, T.; Kim, J. Effect of Hydrogen Derived from Oxygen Source on Low-Temperature Ferroelectric TiN/$Hf_{0.5}Zr_{0.5}O_2$/TiN Capacitors. *Appl. Phys. Lett.* **2019**, *115*, No. 182901.

(44) Ryu, H.; Wu, H.; Rao, F.; Zhu, W. Ferroelectric Tunneling Junctions Based on Aluminum Oxide/ Zirconium-Doped Hafnium Oxide for Neuromorphic Computing. *Sci. Rep.* **2019**, *9*, No. 20383.

https://doi.org/10.1021/acsomega.3c01561
ACS Omega 2023, 8, 18180−18185